A Neuron-Benign Microfluidic Gradient Generator for Studying the Response of Mammalian Neurons towards Axon Guidance Factors

Nirveek Bhattacharjee[*], **Nianzhen Li**[*], **Thomas M. Keenan**, and **Albert Folch**
Department of Bioengineering, University of Washington, 1705 NE Pacific Street, Seattle, WA 98195

Abstract

Investigation of biochemical cues in isolation or in combinations in cell culture systems is crucial for unraveling the mechanisms that govern neural development and repair. The most widely used experimental paradigms that elicit axon guidance in vitro utilize as the source of the gradient a pulsatile pipette, transfected cells, or a loaded gel, producing time-varying gradients of poor reproducibility which are not well suited for studying slow-growing mammalian cells. Although microfluidic device design have allowed for generating stable, complex gradients of diffusible molecules, the flow-induced shear forces in a microchannel has made it impossible to maintain viable mammalian neuronal cultures for sufficiently long times. In this paper, we describe axonal responses of mouse cortical neurons in a "neuron-benign" gradient-generator device based on an open chamber that can establish highly stable gradients of diffusible molecules for at least 6 hours with negligible shear stress, and also allows the neurons to thrive for at least 2 weeks. Except for the period when the gradient is on, the cells in the gradient are under the same conditions as the cells on the control surfaces, which ensure a consistent set of micro-environmental variables. The gradient stability and uniformity over the cell culture surface achieved by the device, together with our software platform for acquiring, post-processing and quantitatively analyzing the large number of images allowed us to extract valuable information even from small datasets. We report a directed response of primary mammalian neurons (from E14 embryonic mice cortex) to a diffusible gradient of netrin *in vitro*. We infer from our studies that a large majority (~73%) of the neurons that extend axons during the gradient application grow towards the netrin source, and our data analysis also indicates that netrin acts as a growth factor for this same population of neurons.

Introduction

During development, the neuron and its axon have to take numerous decisions starting with the specification of the direction of future growth, path-finding, and finally recognition and connection with the target cell. In the last couple of decades, researchers have discovered a plethora of extra-cellular molecules that can enhance the outgrowth of the neuronal processes and/or instructively attract or repel an axon[1–3]. The concerted action of attractive and repulsive cues acting on the axonal growth cone, in a contact-dependent manner or via secreted factors, controls the rate and direction of its outgrowth. The growth cone senses contact-guidance factors through cell-adhesion receptors (integrins, cadherins, CAMs, etc)[4,5] and long-range diffusible guidance factors (netrins, semaphorins, ephrins, slit, etc)[6–8] through unique, specialized receptors, and integrates all the stimuli to produce growth and

Corresponding Author Details: Albert Folch, Associate Professor of Bioengineering, University of Washington, William H. Foege Building, Rm. N430-N, 3720 15th Ave NE, Campus Box 355061, Seattle, WA 98195, Phone: (206) 685-2257; Fax: (206) 685-3300, afolch@u.washington.edu.
[*]These two authors contributed equally to the work

motility. Many of these guidance mechanisms and receptors are evolutionarily conserved from simple organisms like *C.elegans* and *Drosophila* to higher vertebrates, like mammals[9].

In order to investigate the complex behavior of the axon in response to these guidance factors without interference from whole-organism responses, *in vitro* experiments with explants[10] as well as dissociated primary neuron cultures[11] have been extensively used. Although convenient and robust, the explant culture system does not allow for studying single-cell responses. In dissociated cultures, individual neurons can be stimulated by the periodic release of soluble guidance factors from a manipulator-controlled micropipette placed (in the most widely cited protocol) at a 45° angle relative to the previous growth cone navigation direction[11]. The growth cone turning and growth responses are measured by turning angle and elongation distance, respectively. However, in both of these methods above, the gradient never reaches equilibrium, cannot be accurately quantified (as it depends on the initial ejection of a plume-shaped volume, exact pipette size, etc.), and therefore cannot be easily reproduced.

Microfluidic technology has emerged in the past few years as an attractive strategy to create stable, quantifiable and reproducible soluble gradients of biomolecules in fluidic microenvironments at a scale suitable for cellular studies[12]. Moreover, microfluidics allows for running many experiments in parallel under the same conditions, thereby improving the statistical significance of the data obtained. Generally, these devices are made by molding an elastomer, like poly(dimethyl siloxane) (PDMS), against a micro-fabricated template, which is made by standard photolithographic patterning of a photo-polymerizable epoxy (SU-8) on silicon wafer. Conveniently, PDMS is a biocompatible, optically transparent, gas-permeable polymer and therefore ideal for cellular studies.

Many microfluidic devices have been designed to create stable steady-state or dynamic gradients with precise control over the shape, slope and composition of the gradient, by taking advantage of the deterministic nature of fluid flow (laminar flow) in microchannels. One of the more popular designs, by Dertinger and Whitesides[13], based on splitting and recombining flow multiple times to create a gradient, has been adopted by several groups, for example to study neutrophil migration [14], neural stem cell differentiation[15], and breast cancer cell chemotaxis [16]. The Dertinger-Whitesides device, however, suffers from some limitations that make it unsuitable for primary mammalian neuron culture: (a) the gradient can only be generated under a fast flow, thereby exposing the cells to shear and drag forces[17] that can potentially injure and detach the cells and, over time, induce more subtle alterations to intracellular signaling (bias of neutrophil migration towards downstream has been reported[17]); and (b) the gradient can only be generated within an enclosed channel, which limits gas/nutrient exchange, thereby adversely affecting the viability of cells for long-term cultures. Clearly, the cells must be exposed to flow even in the absence of the gradient to preserve viability – a real challenge for mammalian neurons that require ~2 days of recovery after isolation prior to establishing the gradient. There have been other designs[18–21] that have incorporated cell-laden gels inside microfluidic channels, in order to minimize shear-induced damage to cells caused by flow. A recently-described microfluidic device incorporated glass micro-wells and deposited *Xenopus* neurons (fast-growing, non-mammalian) in these wells to shield them from flow-induced shear, thereby increasing cellular viability[22]; it is not known whether this approach is suitable for slow-growing, mammalian neurons. Alternatively, there have also been attempts to study axon guidance in response to insoluble factors by micro-patterning the guidance molecules onto the substrate in stripes interspersed with cell-permissive proteins (in what is popularly known as the "stripe" assay). This approach has been used to direct the growth of rat hippocampal neurons to surface-bound gradients of laminin[23] and chick temporal retinal neurons to gradients of ephrin A5[24]. Although easy to fabricate, these gradients or patterns cannot be altered once

formed, and they are also prone to eventual degradation by protein elution or by cell-secreted proteases. Electroactive self-assembled monolayers[25] also show great promise to produce dynamic gradients on cell culture substrates for axon guidance but require chemistry expertise uncommon in biological laboratories.

In this paper we present a neuron culture platform based on a recently-developed microfluidic device that can generate gradients in an open reservoir[26], with negligible flow and therefore minimal shear-stresses on the cells, which makes it an ideal "neuron-benign" platform. We demonstrate the long-term stability of a gradient of the diffusible guidance molecule netrin and present our first data showing mammalian primary cortical axon responses to netrin. Netrins are a small family of diffusible proteins of ~600 amino acids containing some homology to the ECM protein laminin. They are expressed in various locations in the CNS, and are well known for their conserved role in attracting commissural axons to the midline[27,28]. They also function in other attractive axon guidance pathways, such as the selection of *Drosophila* muscle targets[27] and the guidance of mammalian retinal axons[29,30] and cortical efferent axons[31]. Netrin-induced attraction is mediated by the DCC family of receptors that include Frazzled in *Drosophila*, UNC40 in *C. elegans*, and DCC and neogenin in vertebrates[32]. Netrins can also act as chemo-repulsive signals by binding with a second class of receptors of the UNC5 family in *C. elegans* and *Drosophila* and their three vertebrate homologues (UNC5H1–H3). *In vitro*, netrin attraction via DCC receptors can be switched to repulsion by the association of cytoplasmic P1 domain in DCC and the DCC-binding (DB) motif in UNC5[33]. Recent genetic experiments in *Drosophila* suggest that long-range chemo-repulsion by netrins is mediated by UNC5/DCC receptor complexes, whereas short-range repulsion is mediated by UNC5 alone or with another co-receptor[34]. Despite numerous evidences of the role of netrin on axon growth and guidance *in vivo* and in lower organisms, to the best of our knowledge, there has not been a demonstration of the effect of netrin on dissociated mammalian neurons, most likely because of the neuron response times involved and the gradient stability requirements. Here we report for the first time the response of dissociated mammalian primary cortical neurons to a diffusible gradient of netrin in the absence of any other protein growth factors. The fact that the responsiveness of these delicate neurons has not been detected so far indicates that there is a growing need for microfluidic neuron culture systems where the cell culture conditions are accurately controlled. This experimental platform consisting of the neuron-benign, reproducible gradient generator and the software for quantitative analysis of the acquired data therefore holds a huge potential to unravel the complex mechanisms of axon growth and guidance in response to soluble gradients of a single or multiple diffusible biochemical cues.

Experimental

Fabrication

The basic method of fabrication of the micro-jets device is conceptually similar to that described in an earlier paper[26], with a few key differences as explained below. Briefly, the device is fabricated with the biocompatible elastomer poly(dimethyl siloxane) (PDMS) using a previously developed technique for contact-transferring thin PDMS microstructures that we term "exclusion molding"[35]. A three-layer mold is fabricated integrally in the photosensitive (and e-beam-sensitive) epoxy, SU-8 (Microchem, Newton, MA) using electron-beam lithography (for the microjets features, 2.5 μm-high) and standard photolithography for the other two features (45 μm and 66 μm high, respectively). PDMS is then applied to the mold and excluded from the surface of the tallest features of the mold by compressing them against a polyester sheet (Scotchpak™, 1002 Release Liner, 3M™, St Paul, MN) supported on a glass slide. Conveniently, after the PDMS cures and the polyester sheet is peeled off from the mold, the PDMS structure remains adhered to the polyester sheet, so the PDMS can be transferred to a surface for alignment and bonding with minimal

distortion[35]. Finally, the PDMS structure is exposed to oxygen plasma and bonded onto glass (PDMS does not bond to polyester, so it transfers from the polyester sheet onto the glass).

Modeling and Simulation

In order to better understand the mass and momentum transport within the device, we used finite-element modeling (COMSOL Multiphysics 3.3, Comsol Inc., Burlington, MA) of an infinite slit and solved the Navier-Stokes equation for incompressible fluids (Details on the FEM model have been described in Keenan et al[26]).

Neuron isolation and chamber loading

E14 mouse embryos were harvested from timed pregnant white Swiss Webster female mice (ATL-Harlan, Kent, WA) in accordance with a protocol approved by the University of Washington Animal Care and Use Committee, and decapitated in ice-cold, oxygenated artificial cerebrospinal fluid (ACSF; in mM: NaCl 119, KCl 2.5, MgCl2 1.3, CaCl2 2.5, NaH2PO4 1, NaHCO3 26.2, glucose 11). Cortical cell cultures were prepared using protocols described before[36–39]. After mechanical dissociation, cells were plated on poly-D-lysine (Sigma Aldrich, St Louis, MO) coated glass substrates on which the micro-jets device has already been bonded, at a density of $100/mm^2$ in culture medium containing Neurobasal medium (Invitrogen, Carlsbad, CA) supplemented with B-27 (1X) (Invitrogen), 100 U/mL penicillin–streptomycin (Invitrogen) and 0.5 mM Gluta-Max (Invitrogen). Given the size of the cell chambers, a total cell suspension volume of ~50 μL is enough to load the chamber, which is usually done under a standard light microscope. In order to ensure that no bubbles get trapped in the chambers prior to loading cells, we prime the entre device with Neurobasal media and degas it in a vacuum chamber for about 30 minutes. Once the cells are ready to be plated, most of the media from the chambers is aspirated out, leaving only a tiny volume (~10 μL), so that there is fluidic continuity in the chamber, which eliminates the chances of trapping a bubble. The cells were allowed to attach onto the substrate for 24 hours before the gradient of netrin was introduced.

Gradient imaging

In order to test the stability of the gradients generated by the device, 1 mM fluorescein (Sigma Aldrich, St Louis, MO) mixed with 45 mM Orange G (Sigma Aldrich) was added to one of the side microchannels (the "source"), while the rest of the reservoir and the other microchannel (the "sink") was filled with 45 mM Orange G. The source and the sink microchannels were pressurized (~0.4 to 1.6 psi) leading to fluid being ejected (~40 – 150 pL/min) at the micro-jet locations. Since the pressure changes were done manually, which introduced slight jitter in the images at that point in the experiment, the two images after pressurization were rejected from the analysis. Gradients of netrin were generated by adding netrin-1 (R&D Systems, Minneapolis, MN) at 200 ng/mL to the source microchannel, while having Neurobasal medium in the reservoir and the sink microchannel.

Cell imaging

Long-term imaging of the neurons in the device was made possible by placing the device in an environmental chamber, custom-built to envelope the sample stage of our inverted fluorescence Nikon TE2000 microscope. This chamber was heated with hot air to 37°C with an ultra-silent Nikon air blower. The center region of the stage (where the device was placed) was enclosed by a smaller plexiglass chamber, which contained an inlet and an outlet for perfusion with humidified, pre-warmed 5% CO_2 (humidification and warming of the CO_2 is done by bubbling of 5% CO_2 through a bottle that is kept inside the large environmental chamber, which is equilibrated at 37 °C). Brightfield images were acquired

every 15 minutes with a 12-bit cooled CCD camera (ORCA ER, Hamamatsu, Japan). Metamorph software (Molecular Devices, Sunnyvale, CA) was used to control the movement of the stage, the Z-focusing drive, shutters and the camera. After the experiment, the series of images were registered, processed, and the axon tips tracked using Image Processing tools in Metamorph. Quantitative analysis of the images was done by writing programs in MATLAB, using the Image Processing and Statistical Analysis toolboxes.

Results

Device Operation

As seen in the schematic (Fig. 1A), the microfluidic device (based on a previous design[26], with key modifications) contains an open reservoir 66 μm-deep and 200 (or 500) μm-wide. Two 45 μm-high and 100 μm-wide microchannels serve as "source" (C = C_0 = 200 ng/mL) and "sink" (C = 0) manifolds of netrin to deliver fluids to two arrays of 25 μm-long, 10 μm-wide × 2.5 μm-high microchannels on either side of the reservoir. The small 10 μm × 2.5 μm openings in the reservoir are termed the "micro-jets". We first characterize the stability and profile of gradient formation in the micro-jets device. By constantly replenishing the micro-jet outlets with fresh gradient fluids, two constant concentration boundaries are established in the cell culture area; hence, a steady-state gradient forms at the surface level (even if the air-fluid interface never reaches equilibrium). Equilibration times (arbitrarily defined as reaching 95% of asymptote at the center point of the chamber) range between 2–5 min (a time interval negligible compared to detectable axon growth) depending on ejection pressures and are fastest at the cell culture surface level (a consequence of the fact that the surface is the shortest line between the micro-jets). Moreover the equilibration time is virtually independent of the molecular weight of the species (at least in the tested range of MW = 3–70 kDa), because the gradient is primarily equilibrated by convection[26]. Hence adding a fluorescent tracer to the signaling molecule's solution allows for quantitative visualization of the invisible gradient even if the tracer and the signaling molecule's diffusivities are very different.

While the air-fluid interface occasionally suffers from instabilities, the problem is least pronounced at the cell culture surface level because of the no-slip condition at the fluid-surface interface[40]. The surface gradient is a more accurate indication of what cells sense. We have adapted an imaging protocol for regular epifluorescence microscope to visualize the gradient of fluorescent dyes at the surface of the micro-jets devices[41]. The protocol utilizes the light-absorption spectrum of Orange-G, a non-fluorescent dye that absorbs energy strongly at the excitation wavelength (490 nm) of the dye (fluorescein) or a conjugate of the dye, but weakly at its emission wavelength (540 nm). Therefore Orange-G competes with fluorescein in solution for excitation energy; at 45 mM (with a 0.6 NA objective), it results in an effective penetration length (at which the excitation intensity is 1/e times the incident intensity) of ~4.9 μm for fluorescein as calculated from Beer-Lambert law. Since the excitation decays exponentially from the surface, 95% ($1-1/e^3$) of the fluorescence intensity that we detect comes from the volume that is within ~15 μm of the surface. The measured height of the source and sink microchannels is 45 μm and the height of the microjet channels is 2.5 μm. The fluid height above the cell culture area is ~1 mm; even then the fluorescence intensity at the source microchannel is almost equal to that at the right end of the reservoir, and both are less than twice the intensity at the microjet array, confirming that the fluorescence sampling height is less than 5 μm. Fig. 1B shows an example of surface-level gradient profile of fluorescein in the micro-jets device; Fig. 1C shows the line-scan measurements of fluorescence intensity across the cell culture reservoir over time. The similarity of the lines confirms that the surface gradient in the micro-jets device can be kept stable (within 3–8%) for at least 4 hours. A movie of the gradient stability is available as supplementary information online.

Two salient features of the micro-jets device contribute to make it especially "cell-benign". First, the cells are loaded and kept in an open reservoir prior to application of the gradient – an important consideration for mammalian CNS neurons, usually dissociated in their embryonic stage, that need to recover from the dissociation procedure (over a period of ~2 days). Conveniently, by keeping the neurons in an open environment, the cell culture protocols optimized for traditional non-microfluidic formats (i.e. for standard incubators) do not need to be altered. Second, once the gradient is started, since the fluid is incompressible, after it emerges from the micro-jets it is forced to be directed upwards, away from the cells, towards the air-fluid interface, as confirmed by fluid dynamics simulations (Fig. 1D). Therefore the horizontal component of the fluid velocity in the region within 10 μm of the surface (that contributes to shear forces on cells growing on the surface) is high only at the junction of the micro-jets and the open reservoir, and rapidly decreases with distance towards the center of the reservoir. The FEMLAB simulations in Fig. 1D show that 95% of the surface area experiences shear forces less than 0.7 dynes/cm^2, which ensures that the neurons remain healthy for long periods of time, even after a continuous application of a gradient for at least 20 hours[26].

Response of Primary Neurons to Netrin Gradient in the Device

We have been able to culture primary cortical neurons from E14 embryonic mice cortices in the micro-jets device for 2 weeks, without any adverse effects on the viability of the neurons. Although, dissociated cortical cultures have inherently low viabilities (60–70% of the neurons remain viable after plating in the best of cases), the morphology of the neurons in our chambers (Fig. S1) is comparable to the bright-periphery somas seen in phase-contrast images that are a hallmark of thriving cultures[37–39]. This gives us a long time-window of experimentation, so that we can introduce soluble gradients at a particular developmental stage, as well as study the long-term effects of the gradient on neuronal growth and guidance after its removal. In vivo, cortical neurons are exposed to netrin gradients between E12.5 and E16[31,42,43]; as an approximate model, we subjected the E14 neurons that had matured for 1 day in vitro to a gradient of netrin (as described below in the methods section) for 6 hours and then continued monitoring the neurons for another 12 hours. Fig. 2A shows the population view of the neurons at the beginning and the end of the experimental time period, respectively (a video of the response of the neurons to a gradient of netrin is available as supplementary information), for a representative experiment. For this experiment, out of a total of 113 neurons, only a small percentage of neurons (~10%) grew appreciably during gradient application: 11 neurons experienced a change in the length of the axons greater than 30 μm, which is approximately three times the diameter of the soma of a typical cortical neuron. The percentage is small likely due to the fact that 1) the time window for netrin responsiveness may have been altered by dissociation, and 2) different neurons may be at different stages in their development history when the netrin gradient is applied. Nevertheless, of these 11 neurons, ~73% (8 neurons) had axons growing unequivocally towards the netrin gradient, as determined from the final position of the axon-tip relative to the gradient direction. Fig. 2B plots the trajectories of all the neurons that had axons growing more than 30 μm – the x-axis represents the direction of the netrin gradient and the origin represents the tip of the axon of individual neurons at the start of netrin application. This simple analysis strongly suggests the existence of a population of neurons that are responsive to netrin. The individual micrographs of the 11 neurons, with yellow lines denoting the trajectory during the netrin application period, and the blue lines denoting the trajectory in the post-netrin application period, is included as supplementary information (Fig. S2). It is also to be noted that the netrin-responsive neurons were equally distributed across the gradient chamber (Fig. S1).

Integrated Measurement of Axon Turning

While end-point measurements overlook valuable information that can be extracted from the dynamic process of axon growth in the presence of a gradient (as shown later), measuring the total difference between the initial and final angle of the axon trajectory is a standard way of quantifying axon-turning responses as it integrates the whole history of the experiment. Fig. 3 is a revealing plot of the change in the angle of the axon tip, between the end-points of the experiment. The mean angle of turning is 18.67° towards the source of the gradient. In 8 out of 11 neurons, the axon-tip turned towards the gradient; 6 of which turned by more than 20°, the remaining 5 (including the 3 with negative angular changes) changed by less than 10°. Statistical analysis of this net angular change of the axon trajectories, using the Student's t-test, gives a p-value < 0.05, thereby rejecting the null hypothesis that the net angular change data are a random sample from a normal distribution with zero mean and an unknown variance.

Netrin as a Growth Factor

We were interested in extracting as much temporal information as possible from our single experiment so that the effect of netrin on axon-growth dynamics can be evaluated. (Minimizing the number of experiments is inherently attractive because it minimizes human labor and reagents cost, animal suffering, and data acquisition time.) We analyzed other growth characteristics to see whether the 8 cells that turned towards netrin had any other features in common in order to suggest a netrin-mediated mechanism.. To study the effect of netrin on axon growth dynamics, we measured the magnitude of the axon growth velocity vector, which we term "axon growth speed". The average growth speeds of the individual axons during and after the period of netrin application are plotted in a bar-diagram in Fig. 4A (the neurons have been segregated into the ones that has a net positive turning angle and ones that has a net negative turning angle (as determined from Fig. 3). The instantaneous growth speeds during the entire experimental period, plotted separately for all the neurons, are included as Supplementary Information (Fig. S3). The axon growth speed values for the entire experimental time period are summarized in the bar-diagram of Fig. 4B. We observed statistically significant differences ($p < 0.05$ for neurons growing towards the netrin source, when we used a non-parametric paired, two-sided, signed-rank Wilcoxon test) between the axon growth speed averaged per neuron growing towards the netrin source, during (0 hrs $< t < 6$ hrs) and after (6 hrs $< t < 17.75$ hrs) the application of the netrin gradient. During the time when a netrin gradient was applied, the average growth speed of the axons was approximately 1.5 times the average speed after the gradient was removed. When netrin is removed, the average speed of axons growing towards the gradient is reduced from 25.95 ($+/- 3.07$) to 17.14 μm/hr ($+/- 5.15$) (34% decrease). In other words, during this period netrin essentially acted as a growth factor for the sub-population of neurons that grew towards the gradient. The neurons in which the axons grew away from the gradient also had an increase in growth rate during the netrin application period, but the differences were not statistically significant (using the signed-rank Wilcoxon test).

The Ability to Extend Neurites by Netrin-Responsive Neurons Is Strongly Influenced by the Presence of Contacting Cells

To further investigate possible reasons why some neurons extended their axons in a direction opposite to the gradient source, we looked at the immediate neighborhood of the cells. We observed that the cells that sent off axons in the opposite direction were all part of cell clusters, with cell-cell contact possibly predisposing the extension of an axon from the side of the cell body facing away from the gradient source. In order to quantitatively estimate the accessibility of the axon to grow and be observed on the gradient source-facing side of the cell body, we defined and plotted an "accessibility coefficient" for each netrin-responsive neuron (Fig. 5A). We first determined the angular spread of the cell-body

perimeter (as measured from the centroid of the cell) that is not directly in contact with any other cell (Fig. 5B and 5C). The ratio of the angular spread of the contact-free cell body perimeter on the source-facing side of the cell to the total angular spread of the contact-free cell body perimeter was defined as the "accessibility coefficient". This coefficient gave us a measure of the likelihood of the axons to be observed on the source-facing side of the cell. We plotted this ratio for all the 11 neurons that responded to netrin (Fig. 5A; blue circles denote the neurons that had axons turning towards the direction of the gradient, whereas the red circles denote the neurons that had axons turning away from the gradient). Interestingly, we found that for 7 of the 8 axons that turned towards the gradient, the ratio was somewhere in the vicinity of 0.5 (the range being between 0.5 and 0.58), thereby alluding to the fact that in these neurons, the axons had an equal opportunity to grow in any direction. However if we look at the 3 axons that had the final position of their tips in the half facing away from the gradient source, the ratio was significantly lower (0.22, 0.17, 0.36), which quantitatively confirms that they were in fact pre-disposed to grow on the sink-facing side of the cell. This significant characteristic of the experimental data can possibly determine the differences in the two neuron populations.

Growth Dynamics of Netrin-Responsive Neurons

We also asked whether the population of axons attracted towards the netrin source could be distinguished from the population of axons growing away from the netrin source by differences *in their axon growth dynamics* (rather than their more obvious direction of growth). We postulated that, if our method for measuring axon speed is sensitive enough, it should be able to discriminate between a mode of growth that is enhanced by netrin (towards the gradient) and one that is not (against the gradient). In Fig. 6A we overlaid the axon growth speed values as a color map onto the trajectory of the axon tips for all the netrin-responsive neurons. For further parsing of the speed-time data for the netrin-responsive neurons, we divided the entire speed range (consisting of all the speed-values that the axons take during the entire experimental period) into 10 equal bins (from low to high), and plotted a histogram of the speeds for both groups of the netrin-responsive neurons (those growing towards and those growing away from the netrin source) (Fig. 6B). The histogram shows that the trends look similar for both groups of neurons, except in the lowest speed bin (0 to 5.9 μm/hr), where the neurons growing away from the netrin source were observed to grow at that speed 63% more often than the neurons growing towards the netrin source. Note that the plot in Fig. 6B is averaged over the whole duration of the experiment. To investigate whether this difference was constant throughout the experiment or occurred in bursts, we plotted the first bin of Fig. 6B versus time (Fig. 6C), and found out that a) most of the growth recorded in the first bin of Fig. 6B for neurons growing towards the netrin source (blue bars in Fig. 6C) occurs during netrin application (yellow highlight in Fig. 6C), and b) that for the post-netrin application period, the neurons growing away from the source (red bars in Fig. 6C) had frequent growth occurrences at later time points. Representative examples of the speed-maps superimposed on the actual image and trajectory of typical neurons growing towards and away from the source show the existence of low-speed components (left images in Fig. 6D) in later time points (concentration of blue dots away from the soma, see empty arrow in Fig. 6D) for neurons growing away from the gradient, in clear contrast to the ones that are growing towards the source where the low-speed components are concentrated at the earlier time points (coinciding with netrin application), closer to the soma (see filled arrow in Fig. 6D). A similar analysis does not reveal striking differences in the high-speed components (right images in Fig. 6D). We believe that it is the use of a highly stable, "neuron-benign" gradient generator that has enabled the observation of these subtle differences in dynamic growth behavior.

Discussion

We have demonstrated the use of a versatile microfluidic gradient-generating "micro-jets" device to study the response of dissociated mammalian primary neurons to a stable gradient of a diffusible axon guidance factor, netrin, observed over 18 hours. The micro-jets device has several salient features that make it a very attractive tool for basic neuroscience research:

1. The gradient is created on an open surface, just like on the control surface and on the surfaces of previous investigations that have optimized the cell culture conditions for decades (i.e. we take advantage of well-optimized incubator technology which facilitates gas/pH equilibration and humidity stability and minimizes the need for shear-inducing changes of the cell culture media; all of the above contribute to optimize cell viability in an extremely delicate cell type). This is particularly important because the neurons need to be in the device for a day before the gradient is initiated, so as to recover from the isolation procedure, or to grow, mature, differentiate, as dictated by the experiment. Most of the other designs that have been recently reported for the generation of gel-based low-shear gradients[18–22,44] have not been shown to work with primary mammalian neurons, and do not provide open access to the cultured cells. With the micro-jets, the cells in the controls and in the gradients are, up to the moment of the experiment, in the same conditions as in the past experiments in the literature – covered by ~1 mm of Neurobasal medium, which in turn is covered by humidified, CO_2-rich air (i.e. in a traditional commercially-available incubator). By comparison, if the cells had been in a traditional microfluidic chamber, the cell solution would have been separated from the incubator atmosphere by the ceiling of the microchannel and the optimization of cellular viability would most certainly have required further engineering. As a practical consideration for the future, the ability to probe the neurons on an open surface, e.g. by electrophysiology, may enable certain experiments not possible in other microfluidic devices[35].

2. Since only very small amounts of molecules are actually needed to form a gradient, the flow required is ~40–150 pL/min (i.e. the exposure of cells to flow is negligible); moreover, the direction of the flow is primarily upwards towards the air-fluid interface as soon as it leaves the micro-jets[26], thereby not exposing the majority of the neurons to any appreciable and potentially damaging shear stress. Fluid dynamics simulations show that the region susceptible of flow-induced cell detachment is limited to the 5% of the reservoir surface closest to the micro-jets[26]; the cells located in this zone are discarded from analysis. These levels of shear-force are similarly to other flow-based gradient generating devices used for studying the behavior of primary neurons (~0.005 dynes/cm^2)[22]. Moreover, in our device, the cells in either half are subjected to shear forces in opposite directions (as the flows from the sink and the source microjets are in opposite directions) – yet most (netrin-responsive) neurons grow towards netrin; this provides an internal control (not possible in the other reported designs) that essentially rules out any shear-induced turning or retraction of the growth cones.

3. Assuming all the micro-jets are equally pressurized, all cells at a given distance from the reservoir wall will experience the same gradient and concentration, yielding rich statistics in single-cell data even with very small data sets. Since there is no fundamental limit as to how many micro-jets can be operated in parallel, a much larger chamber containing a much larger array of micro-jets could in principle be imaged with an XY automated stage and image stitching.

4. Last but not least, the micro-jets device also allows the user to dynamically and independently control the slope and position of the gradient[45]. Finally, by altering the location and orientation of the micro-jets, more complex multi-gradient cell culture environments should be possible, which is traditionally possible in other microfluidic flow-based devices[13,22].

This study is the first one to show the response of dissociated mammalian cortical neurons to a soluble stable gradient of netrin, demonstrating that netrin alone (in the absence of other protein growth factors) can induce the growth and guidance of axons in mammalian neurons *in vitro*. Since a majority of the neurons in the experiment extended their axons in the direction of the gradient (Fig. 2), or turned towards the gradient (Fig. 3), and also accelerated their growth-rate during netrin application (Fig. 4), we conclude that such a behavior cannot be attributed to mere experimental chance.

It is important to lay emphasis on the fact that we have been able to culture and elicit responses from primary mammalian neurons, whereas other microfluidic devices[22] have been shown to work for *Xenopus* neurons, which are much easier to culture and responds much faster than mammalian neurons. The role of netrin as a growth factor, which becomes evident from the increased average speed of the axons, has been alluded to in some earlier reports on the role of netrin[8] and is consistent with recent studies that suggest that netrin plays a role in neuronal survival[46]. In *C. elegans* HSN motor neurons in vivo, UNC-6/netrin and its receptor UNC-40/DCC play a role in generating, maintaining and orienting asymmetric growth before axon formation. The immature HSN neuron of *C. elegans* breaks spherical symmetry to extend a leading edge toward ventral UNC-6. In UNC-6 and UNC-40 mutants, leading edge formation fails, the cell remains symmetrical until late in development and the axon that eventually forms is misguided. Thus netrin has two activities: one that breaks neuronal symmetry and one that guides the future axon. The conserved actin regulator UNC-34/Enabled, the PH domain protein MIG-10/lamellipodin and lipid signaling direct axon formation in response to UNC-6/netrin[47]. In order to eliminate the possibility of the neuron's age in culture or other factors actually slowing down the axon growth after the removal of netrin, a future experiment needs to be designed where netrin is applied, removed and then re-applied to the neuronal population and the axon growth rate measured. In light of the very recent discovery of netrin-induced DCC-mediated translation in neuronal membranes[48], it seems possible that axons retain a certain "memory" of enhanced growth rate in response to netrin. Further experiments are needed to elucidate the mechanisms of this putative growth-factor memory.

The relatively low percentage of responsive axons can be attributed to a variety of biological as well as man-induced causes, such as the inherent heterogeneity of the neurons harvested from the cortices, cell damage induced by the isolation procedure (e.g. digestion of the netrin receptor by the proteases used for dissociation of the cells), and/or the different developmental stages they might have been in by the time they were subjected to the netrin gradient. However it is clear that of the axons that grew reasonably (3 cell diameters or 30 μm over 18 hours), a significant majority grew towards the netrin gradient. A close inspection of the axons that grew away from the netrin source reveals that for those axons the axon specification was always on the side of the soma opposite to the netrin source, therefore a turn towards the netrin gradient would have required the axon to turn 90–180 degrees to end up in the direction of the gradient; this preference by the axon to grow straight[49] may be stronger than its ability to respond to chemoattraction, at least in these artificial in vitro scenarios. Also there might be competing factors that are secreted by the neighboring neurons, which might have played a role in the final direction that the axon grows in. The analysis of the neurons growing away from the gradient source hints at the influence of other neurons in the decision-making process of the axon specification and

maybe even growth. In sum, it is not surprising that the number of neurons responding to a given gradient is overall low, which justifies the use of a highly stable and cell-benign gradient generator for basic axon guidance investigations.

We believe that the neuron-benign nature of the device makes it attractive for its use to study differentiation of stem cells into neurons and other cell types, since the differentiation process is very tightly regulated by the spatiotemporal gradients of morphogens. The micro-jets device can also be used to study cell migration and chemotaxis, without having to subject the cells to any forces that would otherwise bias the migration path[17] and confound the results. The gradient stability and uniformity over the cell culture surface make the experiment very amenable to quantitative analysis, which makes it ideal for extracting maximum information from small data sets. The user-friendliness and cell-benign nature of this device brings to the non-specialized biology community at large a very versatile platform that should enable an array of studies that require the activation of cells in the presence of a known chemokine gradient, ranging from cell differentiation, cancer cell migration, wound repair or immune response, among other biological phenomena.

Supplementary Material

Refer to Web version on PubMed Central for supplementary material.

References

1. Chilton JK. Developmental Biology. 2006; 292:13–24. [PubMed: 16476423]

2. Song HJ, Poo MM. Nature Cell Biology. 2001; 3:E81–E88.

3. TessierLavigne M, Goodman CS. Science. 1996; 274:1123–1133. [PubMed: 8895455]

4. Ranscht B. International Journal of Developmental Neuroscience. 2000; 18:643–651. [PubMed: 10978842]

5. Skaper SD, Moore SE, Walsh FS. Progress in Neurobiology. 2001; 65:593–608. [PubMed: 11728645]

6. Kolodkin AL. Neuronal Degeneration and Regeneration: From Basic Mechanisms to Prospects for Therapy. 1998; 117:115–132.

7. Kullander K, Klein R. Nature Reviews Molecular Cell Biology. 2002; 3:475–486.

8. Serafini T, Kennedy TE, Galko MJ, Mirzayan C, Jessell TM, Tessierlavigne M. Cell. 1994; 78:409–424. [PubMed: 8062384]

9. Chisholm A, Tessier-Lavigne M. Current Opinion in Neurobiology. 1999; 9:603–615. [PubMed: 10508749]

10. Tessierlavigne M, Placzek M, Lumsden AGS, Dodd J, Jessell TM. Nature. 1988; 336:775–778. [PubMed: 3205306]

11. Song HJ, Ming GL, Poo MM. Nature. 1997; 388:275–279. [PubMed: 9230436]

12. Keenan TM, Folch A. Lab on a Chip. 2008; 8:34–57. [PubMed: 18094760]

13. Dertinger SKW, Chiu DT, Jeon NL, Whitesides GM. Analytical Chemistry. 2001; 73:1240–1246.

14. Jeon NL, Baskaran H, Dertinger SKW, Whitesides GM, Van de Water L, Toner M. Nature Biotechnology. 2002; 20:826–830.

15. Chung BG, Flanagan LA, Rhee SW, Schwartz PH, Lee AP, Monuki ES, Jeon NL. Lab on a Chip. 2005; 5:401–406. [PubMed: 15791337]

16. Saadi W, Wang SJ, Lin F, Jeon NL. Biomedical Microdevices. 2006; 8:109–118. [PubMed: 16688570]

17. Walker GM, Sai JQ, Richmond A, Stremler M, Chung CY, Wikswo JP. Lab on a Chip. 2005; 5:611–618. [PubMed: 15915253]

18. Cheng SY, Heilman S, Wasserman M, Archer S, Shuler ML, Wu MM. Lab on a Chip. 2007; 7:763–769. [PubMed: 17538719]

19. Shamloo A, Ma N, Poo MM, Sohn LL, Heilshorn SC. Lab on a Chip. 2008; 8:1292–1299. [PubMed: 18651071]

20. Vickerman V, Blundo J, Chung S, Kamm R. Lab on a Chip. 2008; 8:1468–1477. [PubMed: 18818801]

21. Mosadegh B, Huang C, Park JW, Shin HS, Chung BG, Hwang SK, Lee KH, Kim HJ, Brody J, Jeon NL. Langmuir. 2007; 23:10910–10912. [PubMed: 17910490]

22. Wang CJ, Li X, Lin B, Shim S, Ming GL, Levchenko A. Lab on a Chip. 2008; 8:227–237. [PubMed: 18231660]

23. Dertinger SKW, Jiang XY, Li ZY, Murthy VN, Whitesides GM. Proceedings of the National Academy of Sciences of the United States of America. 2002; 99:12542–12547. [PubMed: 12237407]

24. von Philipsborn AC, Lang S, Loeschinger J, Bernard A, David C, Lehnert D, Bonhoeffer F, Bastmeyer M. Development. 2006; 133:2487–2495. [PubMed: 16763203]

25. Yousaf MN, Houseman BT, Mrksich M. Angewandte Chemie-International Edition. 2001; 40:1093.

26. Keenan TM, Hsu CH, Folch A. Applied Physics Letters. 2006; 89:114103.

27. Mitchell KJ, Doyle JL, Serafini T, Kennedy TE, TessierLavigne M, Goodman CS, Dickson BJ. Neuron. 1996; 17:203–215. [PubMed: 8780645]

28. Serafini T, Colamarino SA, Leonardo ED, Wang H, Beddington R, Skarnes WC, TessierLavigne M. Cell. 1996; 87:1001–1014. [PubMed: 8978605]

29. de la Torre JR, Hopker VH, Ming GL, Poo MM, Tessier-Lavigne M, Hemmati-Brivanlou A, Holt CE. Neuron. 1997; 19:1211–1224. [PubMed: 9427245]

30. Deiner MS, Kennedy TE, Fazeli A, Serafini T, TessierLavigne M, Sretavan DW. Neuron. 1997; 19:575–589. [PubMed: 9331350]

31. Metin C, Deleglise D, Serafini T, Kennedy TE. Development. 1997; 124:5063–5074. [PubMed: 9362464]

32. Yu TW, Bargmann CI. Nature Neuroscience. 2001; 4:1169–1176.

33. Seeger MA, Beattie CE. Cell. 1999; 97:821–824. [PubMed: 10399909]

34. Keleman K, Dickson BJ. Neuron. 2001; 32:605–617. [PubMed: 11719202]

35. Hsu CH, Chen CC, Folch A. Lab on a Chip. 2004; 4:420–424. [PubMed: 15472724]

36. Banker, G.; Goslin, K. Culturing Nerve Cells. MIT Press; Massachusetts: 1998.

37. Brewer GJ. J Neurosci Res. 1995; 42:674–683. [PubMed: 8600300]

38. Fedoroff, S.; Richardson, A. Protocols for Neural Cell Culture. Humana Press; 2001.

39. Lesuisse C, Martin LJ. J Neurobiol. 2002; 51:9–23. [PubMed: 11920724]

40. Nguyen, N-T.; Wereley, ST. Fundamentals and Applications of Microfluidics. Artech House; Boston, MA: 2002.

41. Bancaud A, Wagner G, Dorfman KD, Viovy JL. Analytical Chemistry. 2005; 77:833–839. [PubMed: 15679351]

42. Livesey FJ, Hunt SP. Molecular and Cellular Neuroscience. 1997; 8:417–429. [PubMed: 9143559]

43. Shu TZ, Valentino KM, Seaman G, Cooper HM, Richards LJ. Journal of Comparative Neurology. 2000; 416:201–212. [PubMed: 10581466]

44. Abhyankar VV, Toepke MW, Cortesio CL, Lokuta MA, Huttenlocher A, Beebe DJ. Lab on a Chip. 2008; 8:1507–1515. [PubMed: 18818806]

45. Keenan TM, Frevert CW, Wu A, Wong V, Folch A. Lab on a Chip. 2010; 10:116–122. [PubMed: 20024059]

46. Tang XL, Jang SW, Okada M, Chan CB, Feng Y, Liu Y, Luo SW, Hong Y, Rama N, Xiong WC, Mehlen P, Ye KQ. Nature Cell Biology. 2008; 10:698–706.

47. Adler CE, Fetter RD, Bargmann CI. Nature Neuroscience. 2006; 9:511–518.

48. Tcherkezian J, Brittis PA, Thomas F, Roux PP, Flanagan JG. Cell.

49. Li N, Folch A. Exp Cell Res. 2005; 311:307–316. [PubMed: 16263111]
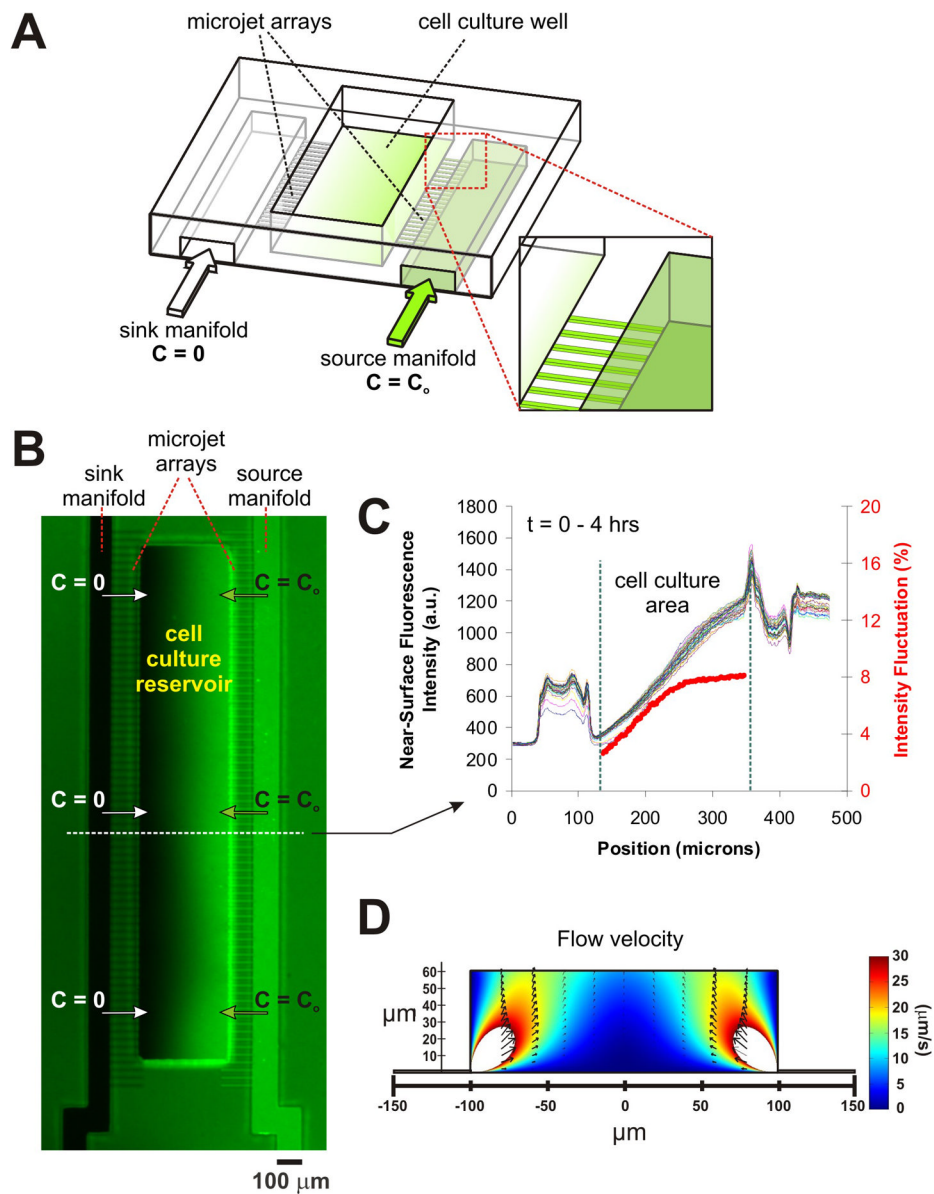
Fig. 1.
The Micro-jets Device: (A) Schematic of the device depicting a central open-surface reservoir (200 μm-wide, 66 μm-deep) that is fed laterally by two microchannels termed "sink manifold" and "source manifold" (each 100 μm-wide), which eject material into the reservoir through an array of small orifices called "micro-jets" (each approx. 10 μm × 2.5 μm cross section); (B) Pseudo-color image showing a representative, 4 hr-long surface gradient profile of fluorescein after the micro-jets are pressurized. The right microchannel ("source manifold") was filled with 45 mM Orange-G and 1 mM fluorescein, while the left microchannel ("sink manifold") and the cell culture reservoir were initially filled with 45 mM Orange-G only. (C) Line-scan measurements of fluorescence intensity across the device over time at the 10 pixel-wide line drawn in (A). The red line depicts the intensity fluctuations (defined as the standard deviation of all the fluorescence values over time observed for any given position of the channel relative to the time-average fluorescence at that position; the first four time points were not included for averaging because the gradient

was still not in steady state). As shown, the gradient remained stable (within 3–8%) for 4 hours. (D) Fluid dynamic simulations plotting the flow velocities in a 60 μm high, 200 μm wide cell-culture reservoir. The arrows show that the flow is mostly directed upwards towards the air-fluid interface.
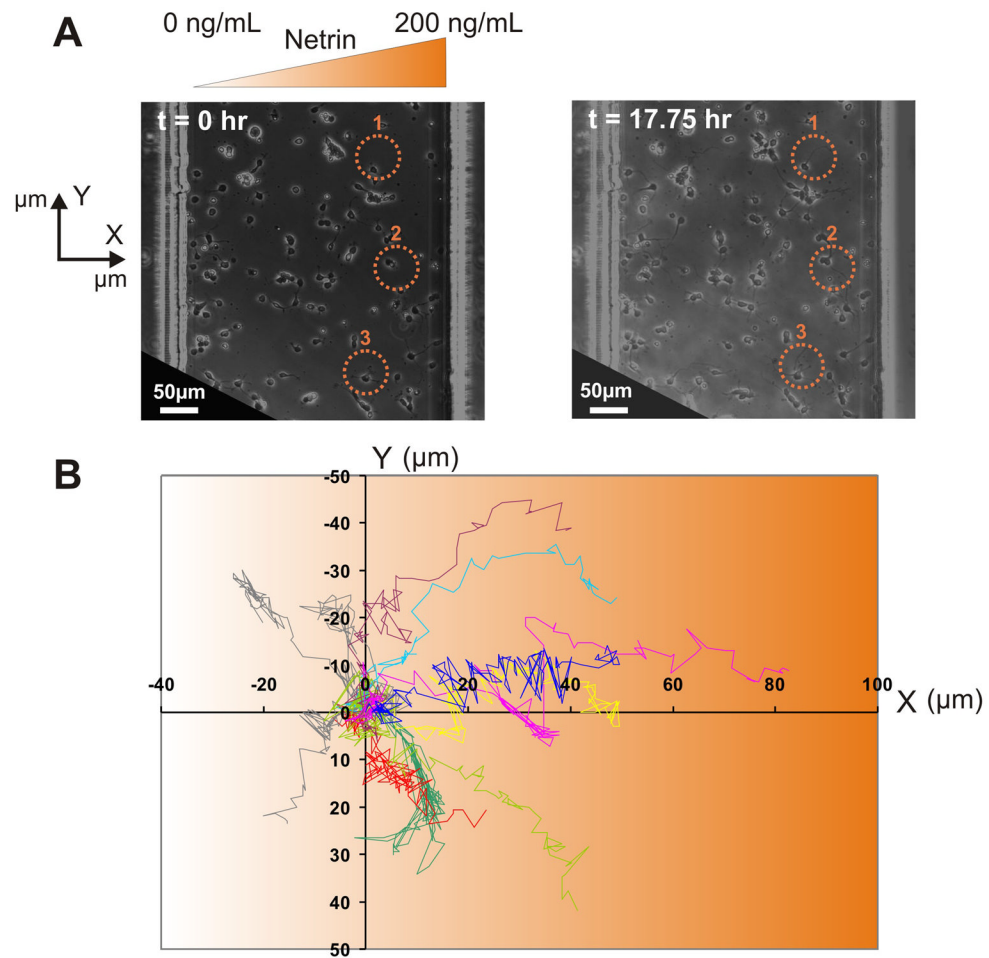
Fig. 2.
Neuronal Response to Netrin: (A) Bright-field image of neurons in the device at the beginning and at the end of the experimental time-period (17.75 hrs). Netrin (0 to 200 ng over a span of 500 µm) was applied for the first 6 hours. Scale bar = 50 µm. (B) Overlay of axon trajectories (normalized to the initial tip positions) from 11 neurons (E14, 1 DIV) during 17.75 hours in one experiment, showing that axons grew towards the netrin gradient.
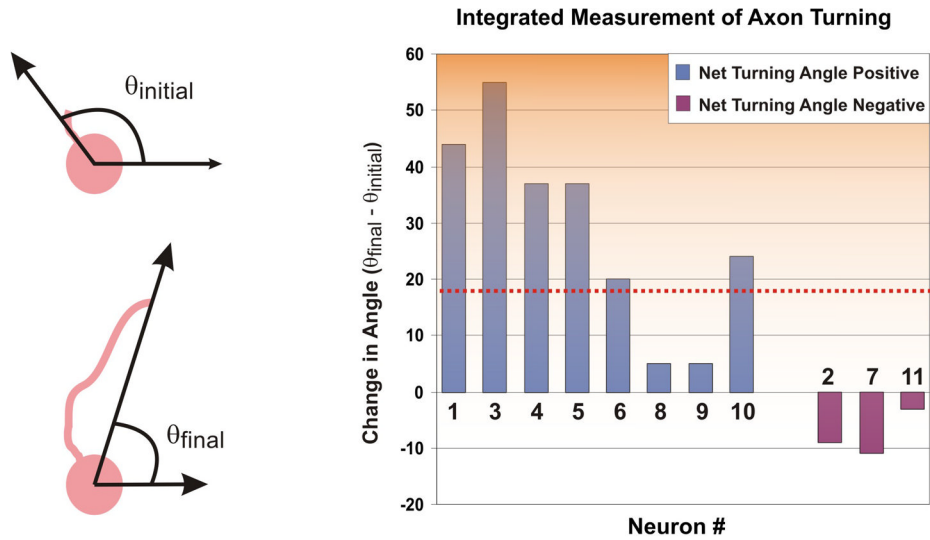
Fig. 3.
Angular Difference of Axon Tip between End-Points: Bar graphs plotting the change in the angle of the axon tip (as measured from the centroid of the cell body, with respect to the gradient direction along the positive y-axis) between the end-points of the experiment. The neurons are grouped according to whether they had a net positive (left 8 "blue" bars) or negative (right 3 "purple" bars) turning angle. The red dotted line represents the mean (18.7°) angle ($p < 0.05$ using Student's t-test).
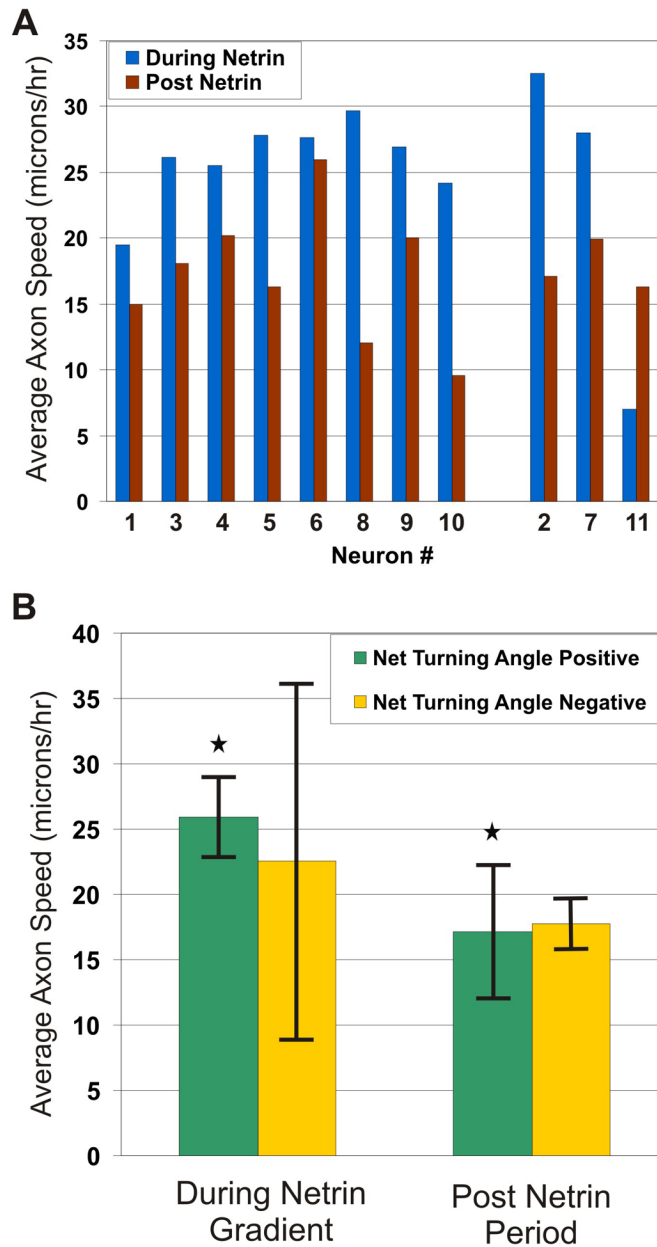
Fig. 4.
Netrin as a Growth Factor: (A) Bar graph plotting the average speed of all the individual axons during netrin gradient application (blue) and after the removal of the gradient (red). The neurons are grouped into ones that had a net positive turning angle (left 8 bars) and ones that had a net negative turning angle (right 3 bars), as determined from Fig. 3 (B) Bar graphs plotting the average normalized speed of the axon tips (magnitude of the axon growth velocity vector) during netrin gradient application, after removal of the gradient, plotted separately for the axons that turned in the direction of the gradient (green, n = 8) and the ones that turned away from it (yellow, n = 3). Error bars in the graph correspond to one standard error above and below the average. * = p-value < 0.05, using non-parametric paired, two-sided, signed-rank Wilcoxon test.
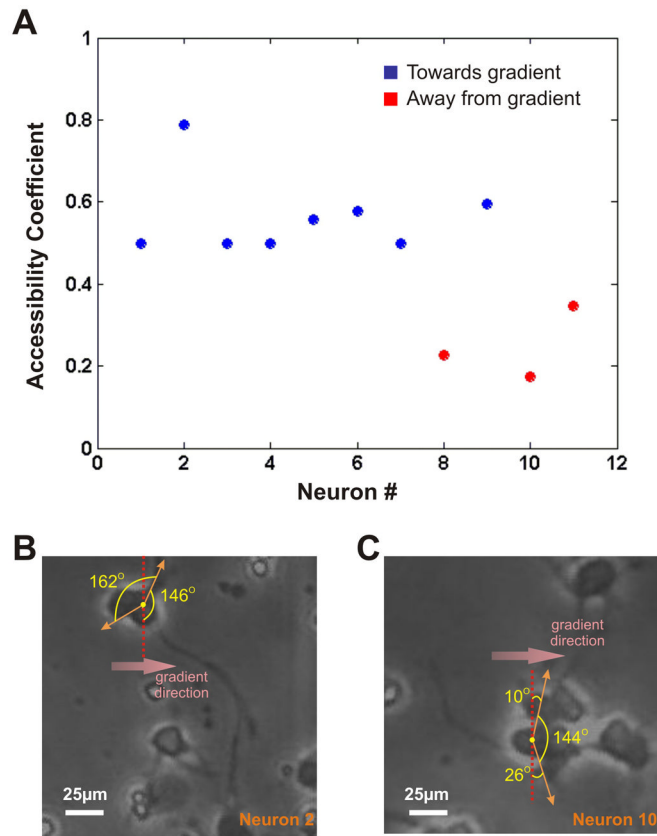
Fig. 5.
Axonal Responses in the Direction of the Gradient Source: (A) Plot of the accessibility coefficient (defined as the ratio of the angular spread of contact-free cell body perimeter on the source-facing side of the cell to the total angular spread of contact-free cell body perimeter) of all the neurons responding to netrin. Blue circles denote the neurons that had axons growing towards the direction of the gradient, whereas the red circles denote the neurons that had axons turning away from the gradient. (B) and (C) Schematics of the accessibility coefficient calculations for sample neurons growing with the final position of their axon tips in the half facing the gradient (#2) and the half facing away from the gradient (#10). Scale Bar = 25 μm.
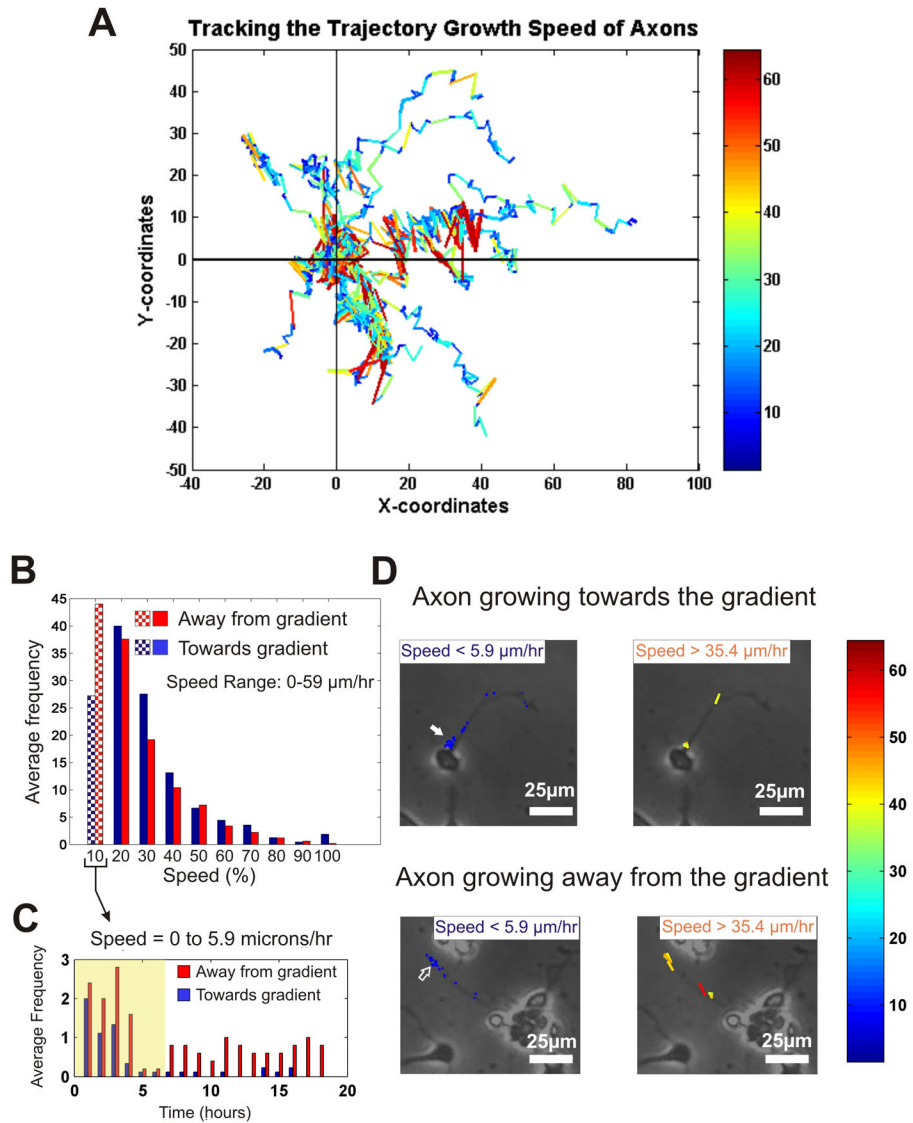
Fig. 6.
Characteristics of Dynamic Behavior of Axons in Response to Netrin: (A) A color-coded axon growth speed map, overlaid on individual axon trajectories – red and blue depict higher and lower speeds, respectively. (B) Histogram of axon growth speeds, divided into 10 equal bins (each bin = 5.9 μm/hr), and averaged, for the axons growing towards (blue) and the ones growing away (red) from the netrin gradient. The shaded region denotes the marked difference between the two populations of neurons. (C) Histogram distribution over time for the lowest speed bracket – 0 to 5.9 μm/hr, corresponding to the leftmost bars in (B) – for both populations of neurons (those growing towards and those growing away from the gradient). The yellow-highlighted region corresponds to the period of netrin gradient application. (D) Color-coded axon growth speed map overlaid on the trajectories of two representative neurons (the upper panel growing towards and the bottom one away from the gradient) showing the distribution of the lower (less than 5.9 μm/hr) and higher (over 37.4 μm/hr) speed bins over time. Note that the distribution of the lower speeds are clustered closer to the soma in cells growing towards the gradient (filled arrows) while they are

clustered away from the soma in cells growing away from the gradient (empty arrows). Scale bar = 25 μm.